Journal of Applied Mathematics & Bioinformatics, vol.8, no.2, 2018, 65-82
ISSN: 1792-6602 (print), 1792-6939 (online)
Scienpress Ltd, 2018

A CAD/CAE Approach For An Efficient Analysis of Contact Mechanics in Rolling Bearings

Stylianos K. Georgantzinos[1]

Abstract

An advanced non-linear finite element method is proposed for effective calculations on the prediction of contact mechanics in rolling bearings. The advanced Augmented Lagrange formulation dealing with non-linear contact problems is adopted. The displacements are approached by using weighted functions, which are called as state variables. Then, the energy equilibrium equations are integrated and are enforced to be equal to zero in a minimization problem of the total potential energy. The bodies in contact, i.e. the bearing elements, are modeled using conventional finite element techniques, in which typical values of mechanical properties are implemented for the bearing materials. Thus, the global stiffness matrix and the corresponding forces and displacement vectors can be assembled. The contact pressure distributions due to the maximum loads of the rolling elements calculated from the numerical solutions. The maximum contact pressures between the rolling elements and raceway obtained

[1] Mechanics Lab, Division of Mathematics and Engineering Studies,
Department of Military Science, Hellenic Army Academy, Vari 16673, Greece.
E-mail: sgeor@mech.upatras.gr

Article Info: *Received* : January 7, 2018. *Revised* : March 2, 2018.
Published online : September 15, 2018.

from the finite element analysis are compared with the contact pressures calculated using analytical solutions available in the open literature. The agreement between the results of the two methods demonstrates the accuracy of the proposed technique.

Mathematics Subject Classification: 74-02; 74M15; 74R99; 74S05
Keywords: Rolling bearings; Contact;

1 Introduction

Bearings are vital machine components in a variety applications of mechanical structures allowing a relative rotational motion of other machine elements like shafts under minimal frictional energy loss. In the design process of a bearing imposed in a cyclic fatigue load, the bearing selection using the classic empiric-analytical machine design process could be characterized as a conservative technique. Furthermore, the detailed examination through experiments [1] of the structural integrity and expected design lives of bearings under actual operational conditions is essentially a timely and economically expensive procedure, since the bearings are needed to be put in a test apparatus rotated under external loads, while extensive testing time is necessary in order to duplicate the failure modes of bearings.

An efficient method to answer the question of the same problem is obviously the development of analytical based solutions. An early attempt, in which the determination of static load distributions from elastic contacts in rolling element bearings, is presented in [2]. In this effort, a method is presented for recording the elastic roll body contacts in the load zone for both radial and thrust rolling element bearings subjected to various static loading conditions. An equation for the prediction of the maximum load on a rolling element based on experimental

observations presented by Stribeck [3], while Harris [4] proposed analytical methods to determine the static load distribution for radial as well as thrust rolling elements. Zhao *et al.* [5] analyzed the relationship between the equilibrium equation of the gyroscopic torque of a rolling element and the coefficient of friction between the rolling element and groove, for the high-speed angular contact ball bearing showing that at a certain rotational speed, the selection of axial force should consider the combined influence of contact force, gyroscopic torque, and coefficient of friction. In a recent study, Xi *et al.* [6] developed a contact trajectory model of ball bearings under the dynamic condition by the means of the development of the integrated multi-body dynamics and multi-freedom kinematics with the multi-interfacial contact mechanics. Other theoretical studies consider investigation on contact simulation of the high angular contact thrust ball bearing [7], contact analysis of deep groove ball bearings in multibody systems [8], the relationship between stiffness and preload for an angular contact ball bearing [9], and the contribution of the deflection of tapered roller bearings to the misalignment of the pinion in a pinion-rack transmission [10].

Hertz theory concerns only local structural deformations of contact areas of bearings and the total deformation of the rolling element, outer ring and inner ring as well as bearing housings cannot be included [11]. Thus, Hertz theory is not precise enough for contact analysis of the ball bearings when the structural deformation is very large. An alternative, which can approach more efficiently the problem, is the Finite Element Method (FEM). Since FEM can be used for efficient predictions, many numerical efforts have been presented in the literature modeling the possible damage or defects that could be developed during rolling bearing operation. Vijay *et al.* [12] presented a three-dimensional Finite Element (FE) modeling approach to include the effects of microstructure topology and material anisotropy in a polycrystalline microstructural bearing steel subject to rolling contact fatigue (RCF) loading. Walvekar *et al.* [13] developed an approach

to simulate 3D experimental (RCF) spalls using a 2D FE model introducing a new concept of dividing the 3D Hertzian pressure profile into 2D sections and utilizing them in a 2D continuum damage mechanics RCF model. Yang *et al.* [14] obtained the contact stress and vibration characteristic curves of rolling bearings establishing numerical models of rolling bearings with different local defect fault poisons. Zhang *et al.* [15] provided insights into the localized stress in a defect zone of the rolling bearings when the rolling elements pass through the defect using an explicit dynamic FE model of a rolling bearing with an artificial round defect in its outer raceway.

In the present work, an advanced non-linear finite element method is proposed for effective numerical calculations that can lead to an advanced prediction of rolling bearing contact mechanics. The bearing parts are modeled using conventional finite element techniques, while the non-linear contact is modeled by the advanced Augmented Lagrange formulation. The displacements in contact area are approached by using weighted functions and the energy equilibrium equations are integrated as well as are enforced to be equal to zero in a minimization problem of the total potential energy. Thus, the global stiffness matrix and the corresponding forces and displacement vectors can be assembled and the equilibrium equations are solved using non-linear techniques. The maximum contact pressures due to the maximum loads of the rolling elements are calculated from the numerical solutions. The results are compared with the contact pressures calculated using analytical solutions available in the open literature.

2 Computational Approach

The subjected load under the operational conditions leads rolling elements to extend their initial contact with raceway. The simultaneous rotation of a supported shaft causes alternative loadings and, thus, the surface fatigue is the expected

failure mode in such an application. In an attempt to predict this failure, contact mechanics analysis is needed. In order to approach numerically this phenomenon, non-linear FE techniques may be required. However, available analytical method should be utilized for reasons of validation and optimization of the proposed FE model. Therefore, the numerical approach of contact problem is presented and is optimized, firstly, comparing classic contact problems, in which Hertz's analytical solution are available and then the optimized models are employed in rolling bearing applications.

2.1 Fundamental equations

As every static problem, in the contact problem between two bodies, the fundamental equations that should be approached by FEM are the stress equilibrium equations described by the following equation

$$\boldsymbol{\nabla\sigma} + \boldsymbol{b} = \mathbf{0}, \tag{1}$$

where $\boldsymbol{\sigma}$ is the stress tensor and $\boldsymbol{b}$ is the vector of the body forces.

Here, the assumption of no one body force is applied ($\mathbf{b} = \mathbf{0}$), since the effect of body forces is negligible comparing to the operational loading. Moreover, the elements are formulated in plane stress conditions ($\sigma_z = \tau_{zx} = \tau_{zy} = 0$). Hence, the equilibrium equations become

$$\frac{\partial \sigma_x}{\partial x} + \frac{\partial \sigma_{xz}}{\partial z} = 0 \tag{2}$$

$$\frac{\partial \sigma_{xz}}{\partial x} + \frac{\partial \sigma_z}{\partial z} = 0 \tag{3}$$

Concerning the materials behavior, here, it is considered to be elastic one, and thus, stress-strain relation is given by the following equation

$$\sigma_i = C_{ij}\varepsilon_j \quad \forall\{i,j\} = \{1,2,\dots,6\} \Leftrightarrow \boldsymbol{\sigma} = [\mathrm{C}]\boldsymbol{\varepsilon} \tag{4}$$

where $[\mathrm{C}]$ is the stiffness matrix, which is the inverse of the compliance matrix $[\mathrm{S}]$,

$$[S] = [C^{-1}] = \begin{bmatrix} 1/E & -\nu/E & -\nu/E & 0 & 0 & 0 \\ -\nu/E & 1/E & -\nu/E & 0 & 0 & 0 \\ -\nu/E & -\nu/E & 1/E & 0 & 0 & 0 \\ 0 & 0 & 0 & 1/G & 0 & 0 \\ 0 & 0 & 0 & 0 & 1/G & 0 \\ 0 & 0 & 0 & 0 & 0 & 1/G \end{bmatrix} \quad (5)$$

where ν is Poisson's ratio, E is the modulus of elasticity and G is the shear modulus of the material.

Considering plane stress conditions and isotropic materials, the linear constitutive equations are given by

$$\sigma_x = \frac{E}{(1+\nu)(1-2\nu)}\left[(1+\nu)\varepsilon_x + \nu\varepsilon_y\right] \quad (6)$$

$$\sigma_y = \frac{E}{(1+\nu)(1-2\nu)}\left[\nu\varepsilon_x + (1-\nu)\varepsilon_y\right] \quad (7)$$

The compatibility equations expressing the relationship between strains and displacements and considering infinitesimal are

$$\varepsilon_{ij} = \frac{1}{2}\left(\frac{\partial u_i}{\partial x_j} + \frac{\partial u_j}{\partial x_i}\right) \quad (8)$$

In the plane stress case the equations become

$$\varepsilon_x = \frac{\partial u_x}{\partial x},\ \varepsilon_y = \frac{\partial u_y}{\partial y},\ \varepsilon_z = \frac{\partial u_z}{\partial z},\ \gamma_{xy} = 2\varepsilon_{yx} = \frac{\partial u_x}{\partial y} + \frac{\partial u_y}{\partial x}. \quad (9)$$

2.2 Numerical approach of static contact problem

In the finite element method, the direct result of the analysis is usually the generalized displacements for elasticity problems. Here, these displacements can be considered as weighted functions and are called *state variables*. The weighted functions are integrated in respect of volumes or areas in 2D problems of contacted bodies. This can be expressed as

$$\delta\mathbf{\Pi} = -\int_A \delta\boldsymbol{\varepsilon}_{\boldsymbol{u}}^{\boldsymbol{T}}\boldsymbol{C}\boldsymbol{\varepsilon}dA + \oint_{\Gamma_\sigma} \delta\overline{\boldsymbol{u}}\boldsymbol{f}^{\Gamma_\sigma}dS = 0, \quad (10)$$

where the first term is the variation of the elastic energy and the second term is the work variation of the surface loads. This integral equation express the minimization of the potential energy of the whole system.

In this way, the static contact problem is transformed to a minimization problem, in which the objective function is the total potential energy $\Pi(\boldsymbol{u})$ of the bodies in contact. Therefore, the problem can be defined as

$$\min \ \Pi(\boldsymbol{u}) \quad (11)$$

$$\text{s.t. } g_j(\boldsymbol{u}) \leq 0, \ j = 1, \dots, n \quad (12)$$

where $\boldsymbol{u}$ is the matrix of the nodal displacement's and the decision variable, while $g_j(\boldsymbol{u})$ describes the n constraints expressing no penetration conditions between the bodies in contact. For these constraints, it is defined that $g_j(\boldsymbol{u}) < 0$ when the bodies are separated, $g_j(\boldsymbol{u}) = 0$ when the bodies are in contact, $g_j(\boldsymbol{u}) > 0$ when the bodies penetrate in each other. The total potential energy $\Pi(\boldsymbol{u})$ for the contact problem between two bodies subjected in small deformations can be described as

$$\Pi(\mathbf{u}) = \Pi_A(\mathbf{u}) + \Pi_B(\mathbf{u}) = \frac{1}{2}\begin{Bmatrix}\mathbf{u}_A\\ \mathbf{u}_B\end{Bmatrix}^T \begin{bmatrix}\mathbf{K}_{\boldsymbol{A}} & \mathbf{0}\\ \mathbf{0} & \mathbf{K}_{\boldsymbol{B}}\end{bmatrix}\begin{Bmatrix}\mathbf{u}_A\\ \mathbf{u}_B\end{Bmatrix} - \begin{Bmatrix}\mathbf{f}_A\\ \mathbf{f}_B\end{Bmatrix}^T \begin{Bmatrix}\mathbf{u}_A\\ \mathbf{u}_B\end{Bmatrix}, \quad (13)$$

where $\mathbf{K}_\mathrm{i}$ are the stiffness matrices, $\mathbf{u}_i$ are the deformation vector of each body and $\mathbf{f}_i$ are the vectors of external loads. For simplicity reasons, the previous variables become $\mathbf{K}$, $\mathbf{u}$ and $\mathbf{f}$ and the total potential energy is given as

$$\Pi(\mathbf{u}) = \frac{1}{2}\mathbf{u}^T\mathbf{K}\mathbf{u} - \mathbf{f}^T\mathbf{u}. \quad (14)$$

Several constrained minimization algorithms can be used to solve the minimization problem of Eq. (2) such as the Penalty Method, the Lagrange Multipliers Method and the Augmented Lagrangian Method (ALM) [16]. In the ALM, the contact constraints are considered in this formulation using penalizing coefficients and Lagrange multipliers, penalizing the non-penetration restrictions violations in the same form of the Penalty method, and solving the constrained

minimization problem through the solution of sequential unconstrained minimization problems with the updating of Lagrange multipliers in the solution process [17].

The ALM is given by

$$L_{aum} = \Pi(\mathbf{u}) + \boldsymbol{\lambda}^t g(\mathbf{u}) + \frac{1}{2} r[g(\mathbf{u})]_+^2, \tag{15}$$

where $[\mathrm{x}]_+$ represents the maximum value of the parameter into the brackets, r is the penalty coefficient $g(\mathbf{u}) = [g_1(\mathbf{u}), g_2(\mathbf{u}), \dots, g_n(\mathbf{u})]$ is the and $\boldsymbol{\lambda}$ is the Lagrange multiplier vector.

The gradient of the ALM function is

$$\nabla L_{aum} = \nabla \Pi(\mathbf{u}) + \boldsymbol{\lambda}^t \nabla g(\mathbf{u}) + [g(\mathbf{u})]_+ \nabla g(\mathbf{u}), \tag{16}$$

which verifies that the penetration restriction satisfies $g(\mathbf{u}^*) = 0$ at the optimum point $\mathbf{u}^*$. In the optimum point, it is that

$$\nabla L_{aum} = \nabla \Pi(\mathbf{u}) + \boldsymbol{\lambda}^t \nabla g(\mathbf{u}^*) = \mathbf{0}, \text{ for every } r. \tag{17}$$

The penalty method coefficients as well as the Lagrange multipliers, can be up to date in a *Newton – Raphson* method in order to obtain a non-linear solution. The contact pressure *P* in ALM is defined as

$$P = \begin{cases} 0, & if\ g < 0 \\ K_n g + \lambda_{i+1}, & if\ g \geq 0 \end{cases} \tag{18}$$

λ_{i+1} is the Lagrange multiplier in $i+1$ iteration, and K_n is the normalized contact stiffness, while

$$\lambda_{i+1} = \begin{cases} \lambda_i + K_n g, if|g| > m \\ \lambda_i, \qquad if|g| \leq m \end{cases} \tag{19}$$

where *m* is the penetration tolerance during the non-linear solution. If the penetration is less than *m*, the Lagrange multipliers are not up-to-date.

The contact problem can be integrated in the potential function adding the contact terms, as calculated by the ALM, into the global stiffness matrix of the model.

2.3 Nonlinear solution

In the FE model the continuum bodies in contact are discretized using conventional 4-noded rectangular linear elements. For reasons of completeness, someone can find their formulation and corresponding elemental stiffness matrix in [18]. As described in the previous section, the stiffness in the contact region varies, and thus, an incremental non-linear procedure is required to approach the solution. The dependence of the stiffness matrix and nodal forces on nodal displacements and their equilibrium is described by the following matrix equation

$$[\mathbf{K}(\mathbf{u})]\{\mathbf{u}\} = \{\mathbf{f}(\mathbf{u})\} \tag{20}$$

The incremental process chosen here is the Newton – Raphson method [19]. Given an initial value, the method generates values that are incrementally converged to the root of the equation based on $\mathbf{u}$ values of the previous iteration for the determination of $\mathbf{K}(\mathbf{u})$,

$$\{\mathbf{u}^{\boldsymbol{r+1}}\} = [\mathbf{K}(\boldsymbol{u})^{r}]^{-1}\{\mathbf{f}\} \tag{21}$$

using the following convergence criterion

$$\{\boldsymbol{u}^{\boldsymbol{r+1}}\} = \{\boldsymbol{u}^{r}\} + \{\Delta\boldsymbol{u}^{r}\} \tag{22}$$

$$|[\mathbf{K}]\{\mathbf{u}\} - \{\mathbf{f}\}| \leq \boldsymbol{\varepsilon}. \tag{23}$$

where r is the number of iteration and $\boldsymbol{\varepsilon}$ corresponds to infinitesimal values. It is clear that the equilibrium between the internal and external forces is checked in every step. After the solution convergence, the nodal displacement calculated in the last iteration can be used in order to calculate the stresses and strains in every node using the following equations

$$\varepsilon_{ij} \cong \frac{1}{2}\left(\frac{\Delta u_i}{\Delta x_j} + \frac{\Delta u_j}{\Delta x_i}\right) \quad \forall\{i,j\} = \{1,2\} \tag{24}$$

$$\sigma_i = C_{ij}\varepsilon_j \quad \forall\{i,j\} = \{1,2,3\} \tag{25}$$

where C_{ij} is the appropriate elastic modulus for each direction.

3 Results and Discussion

3.1 Optimum values of contact parameters

The contact parameter K_n has to be evaluated in the numerical model in order to predict with the optimum accuracy the contact mechanics characteristics and the overall mechanical behavior of rolling bearings. For this reason, some simpler contact problems of elastic bodies, like a cylinder in contact with a plane surface, are used as benchmarks. Different values of contact parameters are tested and the results compared with corresponding ones evaluated by the Hertz contact theory. Then the values fitting best the analytical ones are chosen as the optimal ones and are used for the modelling of the rolling bearing.

3.1.1 Hertz's solutions

The solution for the contact between elastic bodies was derived by Hertz [20]. For the evaluation of the contact pressure p between two faces the

$$\frac{\partial \bar{u}_{z1}}{\partial x} + \frac{\partial \bar{u}_{z2}}{\partial x} = -\frac{2}{\pi E^*} \int_{-\alpha}^{\alpha} \frac{p(s)}{x-s} ds \tag{26}$$

where $\bar{u}_{z1}$ and $\bar{u}_{z2}$ are the displacements of points of the two bodies in the contact region, x is the coordinate in horizontal direction, α is the half contact length with

$$\alpha_{2D} = \left(\frac{3PR}{4E^*}\right)^{1/3}, \quad \alpha_{3D} = \sqrt{\frac{4PR}{\pi E^*}} \tag{27}$$

where R is the cylinder radius, and E^* is the equivalent modulus of elasticity calculated by the following equation

$$\frac{1}{E^*} = \frac{1-\nu_1^2}{E_1} + \frac{1-\nu_2^2}{E_2} \tag{28}$$

where E_i, and ν_i are the modulus of elasticity and Poisson ratio of the two bodies. The solution of Eq. (26) is [20]

$$p(x) = \frac{2P}{\pi\alpha^2}(\alpha^2 - x^2)^{1/2} \tag{29}$$

where P is the applied load. The maximum contact pressure is given by the following equation

$$p_{o2D} = \frac{3P}{2\pi\alpha^2} = \left(\frac{6PE^{*2}}{\pi^3 R^2}\right)^{1/3}, \quad p_{03D} = \frac{2P}{\pi\alpha} = \left(\frac{PE^*}{\pi R}\right)^{1/2} \tag{30}$$

3.1.2 Numerical vs analytical results

Considering the case described in Fig. 1, the FE models are developed and analyzed based on the approach presented in Section 2. Here, the parameters are chosen to be R = 10 mm, and P = 3 kN/mm. The material properties are considered as $E_1 = E_2$ = 200 GPa and $\nu_1 = \nu_2$ = 0.3. Using the same values the contact pressure is calculated using also the analytical method.

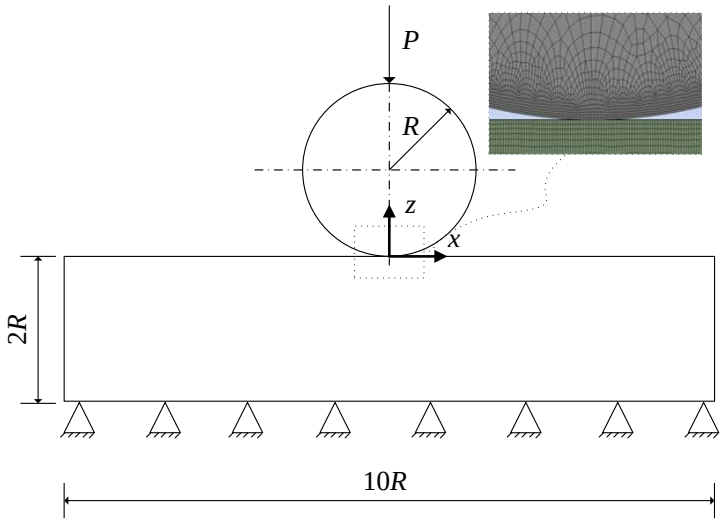

Figure 1: Geometry and meshing details of benchmark contact problem

The first set of tests concerns the meshing optimization in terms of accuracy. The chosen discretization of the continuum bodies, particularly in the contact region is presented in Figure 1. This choice outcomes form the results depicted in Figure 2a, applying the appropriate number of divisions in contact surfaces in

order the numerical solution to converge with the analytical one.

The optimum value of K_n is the main issue optimizing the accuracy of the proposed model. Testing different values, it is observed from Figure 2b that a value K_n = 20, is the appropriate one in order to analytical and numerical solutions converge in terms of p_{max}. Figure 2c reveals that this value is also reasonable in terms of α as well. Therefore, it is concluded that the optimum value of K_n is 20.

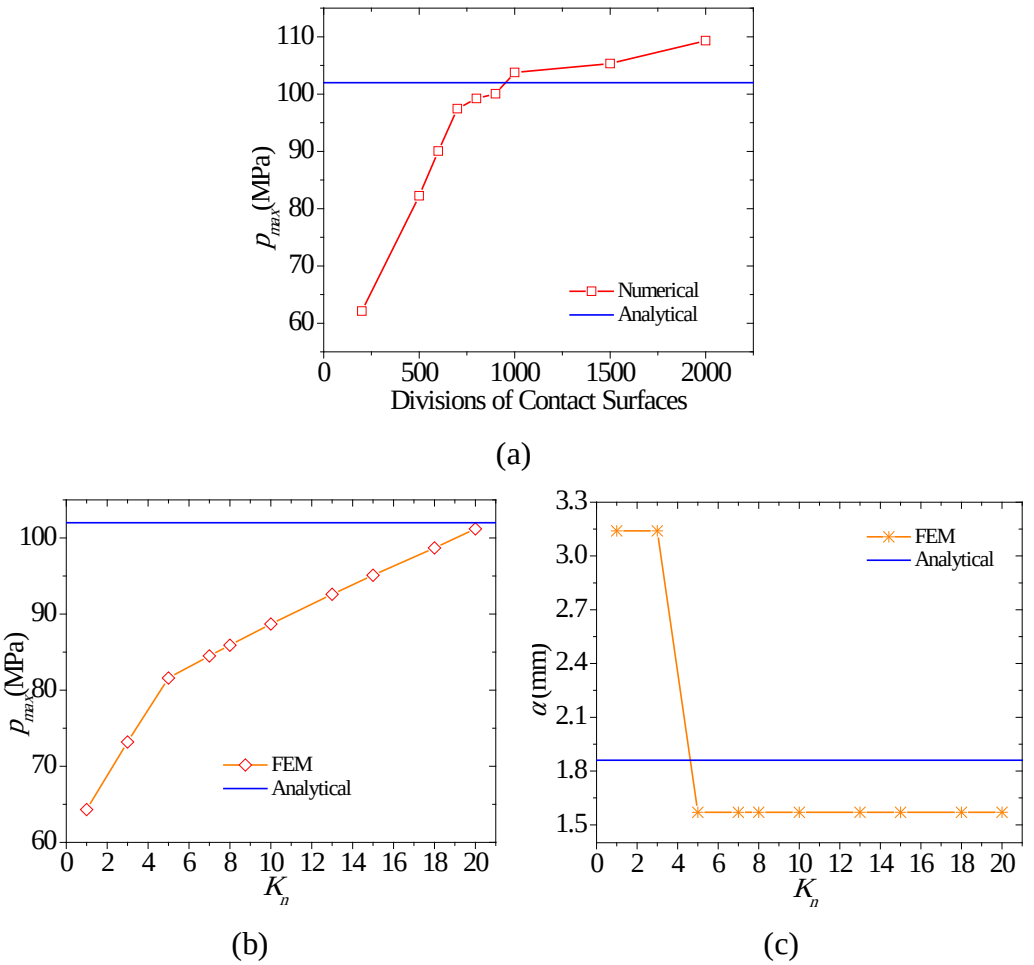

Figure 2: Optimum values of contact parameters in terms of (a) mesh, (b) p_{max}, and (c) α

For a further validation of the optimized model, stress analysis results calculated by the numerical approach and corresponding ones from analytical methods [20] are also compared. This comparison is presented in Fig. 3. It is noticed that a reasonable accuracy between the methods concerning the normal stresses σ_x (Fig. 3a), and σ_x (Fig. 3b) occurs. Therefore, the proposed model can be assumed as a reliable one and may be applied in order to calculate effectively corresponding contact mechanics results in rolling bearings.

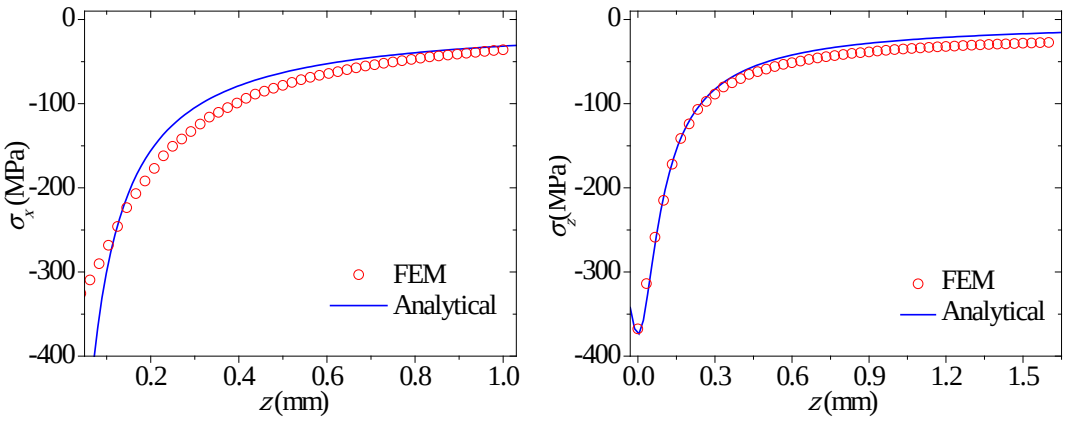

(a) (b)

Figure 3: Normal stress (a) σ_x, and (b) σ_z

3.2 Numerical Solutions in Rollling Bearings

Since, the numerical techniques is now fully defined, a specific roller bearing with 18 rolling elements is analyzed using the proposed procedure. The materials properties are E = 200 GPa, ν = 0.3. In order to examine the accuracy of the present method also in rolling bearings, some analytical calculations are also adopted for reasons of comparisons. The geometry of the specific application and the corresponding model is presented in Fig. 4. The outer diameter of outer ring is

100 mm, its thickness as well the diameter of roller elements is 20 mm.

The boundary conditions of the problem concerns a displacement restriction on the outer surface of the outer ring. The inner ring and the supported shaft are modeled as one body since they are considered to have the same material properties. Here, it is assumed a vertical static load P_{total}, which simulates the loading under operation conditions.

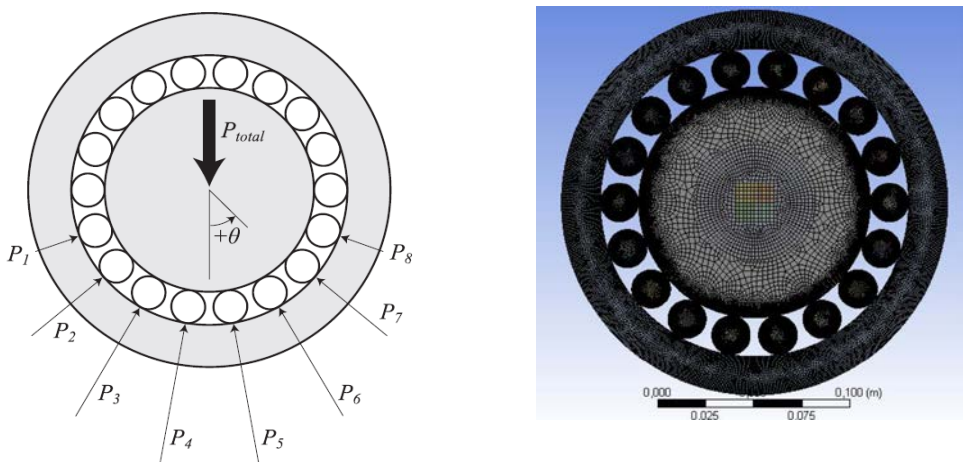

(a) (b)

Figure 4: Roller bearing with 18 rolling elements (a) Geometry, and (b) FE model

Applying P_{total} = 60kN/mm to the numerical model, the non-linear analysis reveals the solution. Fig. 5a presents maximum contact pressure in the contact area of every rolling element according to its angular position. These results are compared with corresponding ones based on Person theory and the analytical modifications found in [21]. A sensible agreement between the methods can be observed. Notice that the discrepancy does not exceed the value of 5% in all cases. Tests and comparisons with different loading magnitudes has given similar results.

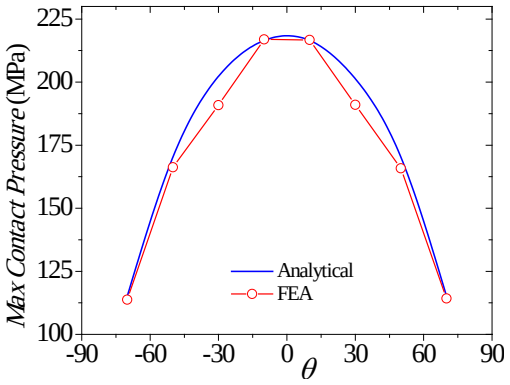

Figure 5: Maximum contact pressure distribution in the roller bearing

Applying a greater loading P_{total} = 600kN/mm, the results are now directed on the stress distribution into the roiling bearing elements. Focused on the rolling element with the maximum contact pressure the normal stresses regarding the local vertical axis of the elements are calculated and are presented in Fig. 6. Comparisons with analytical solutions [21] reveal again the excdllent accuracy of the proposed method.

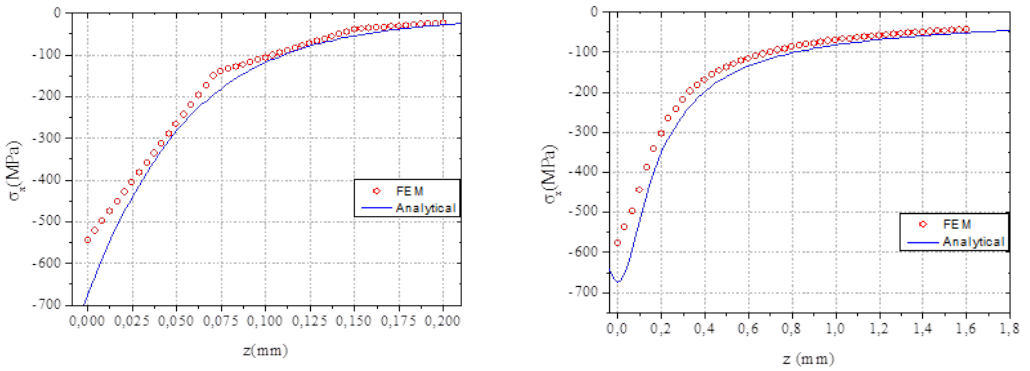

(a) (b)

Figure 6: Normal stresses in the region of rolling element with the highest contact pressure (a) σ_x, and (b) σ_z

5 Conclusion

In this paper, a systematic numerical procedure was developed for an accurate and efficient contact mechanics analysis on rolling elements and cylindrical roller of rolling bearings. The method combines conventional FEM techniques for the rolling element modeling, the ALM, and iterative methods in order to solve the non-linear contact problem. For optimization reasons, simpler contact mechanics problems are firstly analyzed and optimum values of contact parameters are extracted according to the comparisons with analytical methods. In this way, it was clear that the accuracy of the proposed techniques essentially improved. The optimized modeling observations were applied, then, on a specific rolling bearing configuration. The obtained results revealed contact mechanics characteristics like maximum contact pressures. Comparisons with other analytical techniques available in the open literature demonstrated the overall accuracy of the propose procedure on the mechanical analysis of rolling bearing. Based on the present technique, advanced analysis can be also conducted in a future work, since more complicated phenomena like a damage may be inserted in the model, and corresponding accurate predictions may be revealed.

References

[1] E. Houara Komba, F. Massi, N. Bouscharain, G. Le Jeune, Y. Berthie, Y. Maheo, Experimental damage analysis in high loaded oscillating bearings, *Tribology International*, **102**, (2016), 507–515.

[2] R.A. Goodelle, W.J. Derner, and L.E. Root, Determination of static load distributions from elastic contacts in rolling element bearings, *ASLE Transactions*, **14**(4), (1971), 275-291.

[3] B. Jacobson, The Stribeck memorial lecture, *Tribology International*, **36**, (2003), 781–789.

[4] T.A. Harris, *Rolling bearing analysis*, John Wiley and sons, 2001.

[5] C. Zhao, X. Yu, Q. Huang, S. Ge, X. Gao, Analysis on the load characteristics and coefficient of friction of angular contact ball bearing at high speed, *Tribology International*, **87**, (2015), 50-56.

[6] H. Xi, H.Y. Wang, W. Han, Y. Leb, H. Xu, W. Chen, S.N. Xu, F.C. Wang, Contact trajectory of angular contact ball bearings under dynamic operating condition, *Tribology International*, **104**, (2016), 247–262.

[7] H. Wang, S. Dai, Study on contact finite element simulation of the high-angular contact thrust ball bearing, *Computer Simulation*, **1**, (2013), 1–70.

[8] Z. Qi, G. Wang, Z. Zhang, Contact analysis of deep groove ball bearings in multibody systems, *Multibody System Dynmics*, **33**(2), (2015), 115–141.

[9] J. Zhang, B. Fang, Y. Zhu, J. Hong, A comparative study and stiffness analysis of angular contact ball bearings under different preload mechanisms, *Mechanism and Machine Theory*, **115**, (2017), 1–17.

[10] V. Roda-Casanova, F. Sanchez-Marin, Contribution of the deflection of tapered roller bearings to the misalignment of the pinion in a pinion-rack transmission, *Mechanism and Machine Theory*, **109**, (2017), 78–94.

[11] S. Li, A mathematical model and numeric method for contact analysis of rolling bearings, *Mechanism and Machine Theory*, **119**, (2018), 61–73.

[12] A. Vijay, N. Paulson, F. Sadeghi, A 3D finite element modelling of crystalline anisotropy in rolling contact fatigue, *International Journal of Fatigue*, **106**, (2018), 92–102.

[13] A.A. Walvekar, D. Morris, Z. Golmohammadi, F. Sadeghi, M. Correns, A novel modeling approach to simulate rolling contact fatigue and three-dimensional spalls, *Journal of Tribology*, **140**(3), (2018), 031101.

[14] X. Yang, C. Yan, Y. Li, Finite element simulation and experimental study on vibration effect of defect position for cylindrical roller bearing, *International Journal of Control and Automation*, **10**(8), (2017), 1-12.

[15] Z. Zhang, W. Ding, H. Ma, Local stress analysis of a defective rolling bearing using an explicit dynamic method, *Advances in Mechanical Engineering*, **8**(12), (2016), 1–9.

[16] D.P. Bertsekas, Constrained Optimization and Lagrange Multiplier Methods, Academic Press, New York, 1982.

[17] G. Hattori, A.L. Serpa, Contact stiffness estimation in ANSYS using simplified models and artificial neural networks, *Finite Elements in Analysis and Design*, **97**, (2015), 43–53.

[18] K.-J. Bathe, Finite element procedures, Klaus-Jurgen Bathe, 2006.

[19] T.J. Ypma, Historical development of the Newton–Raphson method, *SIAM review*, **37**(4), (1995), 531-551.

[20] K.L. Johnson, K.L. Johnson, Contact mechanics, Cambridge university press, 1987.

[21] J. Lee, J. Pan, Closed-form analytical solutions for calculation of loads and contact pressures for roller and ball bearings, *Tribology International*, **103**, (2016), 187–196.